Water Oxidation by the [Co4O4(OAc)4(py)4]+ Cubium is Initiated by OH– Addition

Water Oxidation by the $[Co_4O_4(OAc)_4(py)_4]^+$ Cubium is Initiated by OH^- Addition

Paul F. Smith[1], Liam Hunt[1], Anders B. Laursen[1], Viral Sagar[1], Shivam Kaushik[1], Karin U.D. Calvinho[1], Gabriele Marotta[2], Edoardo Mosconi[2], Filippo De Angelis[2], and G. Charles Dismukes*[1]

[1]Department of Chemistry and Chemical Biology, Rutgers, the State University of N.J. 610 Taylor Road Piscataway NJ 08854, [2]Computational Laboratory for Hybrid/Organic Photovoltaics (CLHYO), Istituto CNR di Scienze e Tecnologie Molecolari (ISTM-CNR), Via Elce di Sotto 8, Perugia, Italy

Supporting Information Placeholder

ABSTRACT: The cobalt cubium $Co_4O_4(OAc)_4(py)_4(ClO_4)$ (**1A**$^+$) containing the mixed valence $[Co_4O_4]^{5+}$ core is shown by multiple spectroscopic methods to react with hydroxide (OH^-) but not with water molecules to produce O_2. The yield of reaction products is stoichiometric (>99.5%): 4 **1A**$^+$ + 4 $OH^- \rightarrow O_2$ + 2 H_2O + 4 **1A**. By contrast, the structurally homologous cubium Co_4O_4(trans-OAc)$_2$(bpy)$_4$(ClO$_4$)$_3$, **1B**(ClO$_4$)$_3$ produces no O_2. EPR/NMR spectroscopies show clean conversion to cubane **1A** during O_2 evolution with no Co^{2+} or Co_3O_4 side products. Mass spectrometry of the reaction between isotopically labeled μ-^{16}O(bridging-oxo) **1A**$^+$ and ^{18}O-bicarbonate/water shows: 1) no exchange of ^{18}O into the bridging oxos of **1A**$^+$, and 2) $^{36}O_2$ is the major product, thus requiring two OH^- in the reactive intermediate. DFT calculations of solvated intermediates suggest that addition of two OH^- to **1A**$^+$ via OH^- insertion into Co-OAc bonds is energetically favored, followed by outer-sphere oxidation to intermediate [**1A**(OH)$_2$]^0. The absence of O_2 production by cubium **1B**$^{3+}$ indicates the reactive intermediate derived from **1A**$^+$ requires gem-1,1-dihydoxo stereochemistry to perform O-O bond formation. Outer-sphere oxidation of this intermediate by 2 eq. **1A**$^+$ accounts for the final stoichiometry. Collectively, these results, and recent literature (Faraday Disc., doi:10.1039/C5FD00076A and J.Am.Chem.Soc 2015, 12865-12872) validate the $[Co_4O_4]^{4+/5+}$ cubane core as an intrinsic catalyst for oxidation of hydroxide by an inner-sphere mechanism.

Introduction

Sustainable production of hydrogenic fuels requires an abundant source of hydrogen. Water is the ideal source of hydrogen, but must first be cleaved by an energetic process in which 4 strong O-H bonds are broken. Towards this goal, several heterogeneous cobalt oxide catalysts for electrochemical water oxidation have been reported[1–6] and widely applied[7–18]. Rational design of heterogeneous catalysts is difficult, and can significantly benefit from understanding gained from simpler homogenous catalysts. To better understand their basis for catalysis, several molecular cobalt clusters have been synthesized and reported to be active homogenous catalysts[19–29]. Of interest from these are clusters containing a Co_4O_4 "cubane" core[30,31], which is a recurring structural theme among biological and synthetic water oxidation catalysts[32,33]. Many studies have described the properties[34–47] of $Co_4O_4(OAc)_4(py)_4$, **1A**, and $[Co_4O_4(OAc)_2(bpy)_4](ClO_4)_2$, **1B**$^{2+}$(ClO$_4$)$_2$ (Scheme 1).

The synthesis and characterization of cubane **1A** has an extensive history. Oxidation of Co^{2+} acetate by peroxide or peracetic acid was known to give a complex, equilibrating, reaction mixture, until the addition of pyridine allowed isolation of dimeric and trimeric cobalt cations[48]. Cubane **1A**, which is neutral and has high solubility in many solvents, escaped detection from this synthesis until many years later[47]. Other studies targeted formation of the cubane using alternate carboxylates and substituted pyridines to shift the equilibrium[38], though the general synthetic method remained similar. These later reports served as the basis for the preparation of **1A** by several groups including ourselves, who all showed **1A** (and close analogs) to oxidize water (pH 6-8) photochemically and electrochemically[49–55]. DFT calculations suggested energetically accessible routes to catalytic O_2 evolution from model Co_4O_4 cubanes (terminated by water ligands), though nucleophilic attack[56], cross-coupling[57] and geminal coupling[58] mechanisms have been proposed.

Scheme 1. Cubanes: $Co_4O_4(OAc)_4(py)_4$, **1A**, and $[Co_4O_4(OAc)_2(bpy)_4]^{2+}$, **1B**$^{2+}$

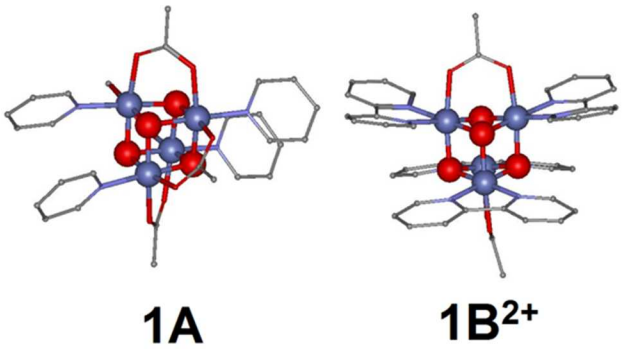

Recently, Nocera et al. provided strong evidence that Co^{2+} impurities remaining from synthesis form the main catalyst when oxidized in phosphate buffer either electrochemically or *via* a Ru^{3+} photo-oxidant[59]. From that report, pristine **1A** was found inactive for electrochemical water oxidation.

While the pure compound was photochemically active, catalysis was ascribed to decomposition products. More recently, Bonchio et al. showed by kinetic studies that **1A** minus an acetate ligand is the most likely intrinsic water oxidation catalyst in the photochemical assay[60]. This derivative is accessible by aging **1A** in water, and additionally shows electrochemical activity.

Herein we show that the oxidized cubium, **1AClO4**, reacts with OH- to release O2 spontaneously without an external oxidant, light or electrolysis potential. The Co4O4 cubane core serves two roles in O_2 evolution: intact **1A**$^+$ serves as an outer sphere oxidant, and as pre-catalyst that forms the reactive intermediate by association with hydroxide. Evidence from mass spectrometry, NMR and DFT calculations of energy minimized structures implicates formation of an association complex via insertion of OH- into a Co-OAc$^-$ bond of **1A**$^+$, forming the first pre-catalytic intermediate, **[1A(OH)]**. This intermediate cannot be oxidized by another 1A$^+$ molecule until a second OH$^-$ inserts in another Co-OAc$^-$ bond, yielding **[1A(OH)$_2$]**^{0}. Isotopic labeling studies establish that terminally coordinated hydroxide ions, but not bridging oxos within the cubane, are the substrates that form O2. Our results on the reactivity of **1A**$^+$ with OH$^-$ agree with those in a recent report that appeared while this manuscript was in review[61] and also provides additional kinetic data that is described in the discussion. Our results are further extended herein by parallel studies of a structurally homologous cubium **1B**$^{3+}$ having only 2 carboxylate chelates in trans configuration and 4 bpy replacing py (Scheme 1). In contrast to **1A**$^+$, the isolated perchlorate derivative, **1B(ClO4)3**, fails to produce O2 when reacted with OH$^-$, suggesting the stereochemistry of the associative hydroxide intermediate involves the gem-1,1-dihydroxo formation from **1A**$^+$ as precatalyst.

Results

Reduction of 1A$^+$ in Presence of Hydroxide.

After performing column chromatography on samples of cubane **1A**, we observed no noticeable water oxidation current above a background glassy carbon electrode in buffered water (0.1 M phosphate buffer at pH 7) (Figure 1), consistent with the pure samples isolated by several groups [59–61] We adapted two literature procedures to synthesize **1A**$^+$: 1) electrochemical oxidation[44], yielding the ClO_4^- salt; 2) chemical oxidation[59], yielding the PF_6^- salt. The following results are all consistent regardless of preparation method.

The EPR spectrum of **1A**$^+$ dissolved in water/acetonitrile glass forming solvent is comparable to the initial report of Britt, et. al.[44] (Figure 2). Specifically, the line shape and Curie temperature dependence indicate a spin S = ½ ground state with an axial g tensor, $g_{\parallel}$=2.06 and $g_{\perp}$=2.28. There is no resolved hyperfine structure from ^{59}Co (I = 7/2, 100% n.a.) and no features at lower field where species of higher spin multiplicity can absorb. The sample (up to 15 mM concentration) exhibits no EPR signal for Co^{2+} or for that matter any paramagnetic impurity.

1A$^+$ as isolated is not water soluble, but dissolves in aqueous solutions of NaOH, N-butylammonium hydroxide, sodium bicarbonate, and sodium carbonate. As monitored by EPR and UV-Vis spectroscopies the addition of any of these hydroxide sources to **1A**$^+$/CH_3CN solutions results in reduction to diamagnetic **1A** (Figures 2 and 3, respectively). Bubbles are released upon this reaction and confirmed as O_2 by Clark electrode, gas chromatography and membrane inlet mass spectrometry (*vide infra*).

UV-Vis titrations indicated 1:1 stoichiometry of cubium to hydroxide completes the reaction (Figure 3, inset, and Figure S1). Given that **1A**$^+$ precipitates from water in the last step of synthesis, no reduction in the presence of water was anticipated, as confirmed by control experiments over the time scale of several minutes (Figure S1). Control measurements without **1A**$^+$ or OH$^-$ produced no measureable O_2 in all these trials.

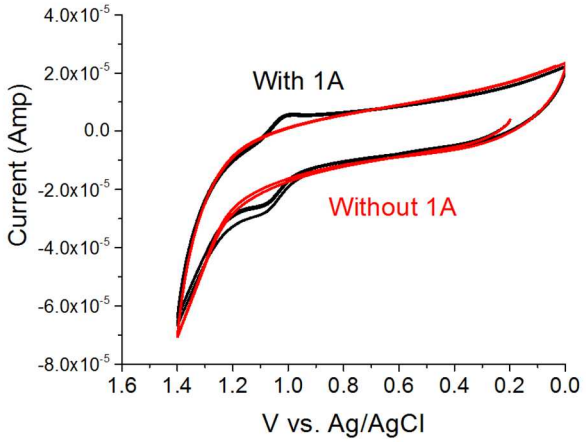

Figure 1. Cyclic voltammograms at a glassy carbon electrode in aqueous phosphate (0.1M, pH 7) with and without 500 µM of **1A.**

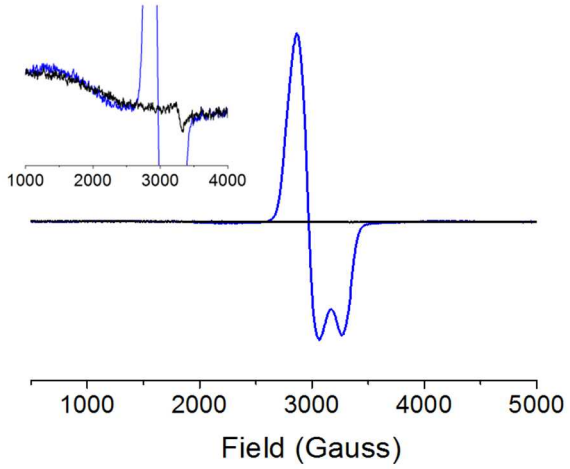

Figure 2. EPR spectrum at 10 K of 15 mM CH_3CN solutions of **1A(ClO$_4$)** without (blue) and with (black) 0.1 M NaOH. **Inset**: 10x expansion from another independent trial. Samples were not degassed.

Gas chromatography was used to quantify the O_2 produced upon complete dissolution of 2-2.5 µmol of **1A(ClO$_4$)** in 10 eq. aqueous NaOH. The amount of O_2 produced was quantitatively consistent with reduction of $4Co^{4+}$ to $4Co^{3+}$ (O_2:**1A**$^+$ ratio of 0.27 ±0.03). NMR integration of the product solution was quantitatively consistent with formation of **1A** as the sole

product (99.5% recovery). Consistent with this result, EPR spectroscopy of solutions of the reaction product showed no identifiable paramagnetic Co^{2+} (Figure 2, black trace); suggesting only Co^{3+} in the product. We did not observe CO_2 or CO in the product gas above GC detection (< 10 nmol, 0.5%), consistent with no oxidation of substrates other than OH^-. Hence, the reaction stoichiometry is given by eqn (1):

$$4\ \mathbf{1A}^+ + 4\ OH^- \rightarrow O_2 + 4\ \mathbf{1A} + 2\ H_2O \qquad (1)$$

As determined by Clark electrode, the method of initial rates indicates that the O_2 evolution reaction is first order in both cubium and OH^- when using one limiting reactant (pseudo-first order conditions) (Figure 4). Rates decrease from linear dependence at $[OH^-]$> 1 mM. A plot of the pseudo-first order constants vs. $[OH^-]$ gives the bimolecular rate constant k= 1.1 $(M*s)^{-1}$ for the reaction, (eqn. 2).

$$d[O_2]/dt = k\ [\mathbf{1A}^+]\ [OH^-]\ ,\ k = 1.1\ /\ M*s \qquad (2)$$

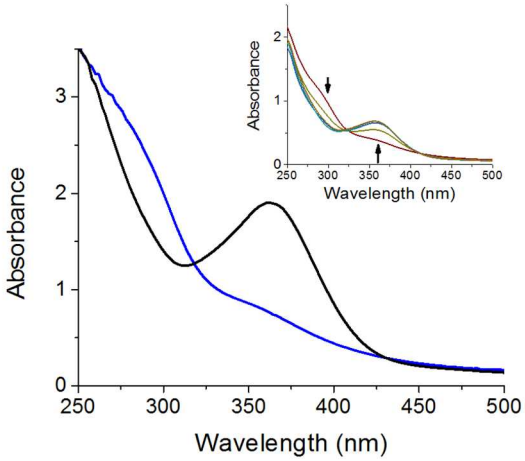

Figure 3. UV-Vis spectra of 170 µM CH_3CN solutions of $\mathbf{1A}^+$ (blue) and **1A** (black). Inset: Spectral changes following addition of 4x 0.5 eq. aliquots of OH^- to 60 µM of $\mathbf{1A}^+$, showing two isosbestic points and no observable intermediates.

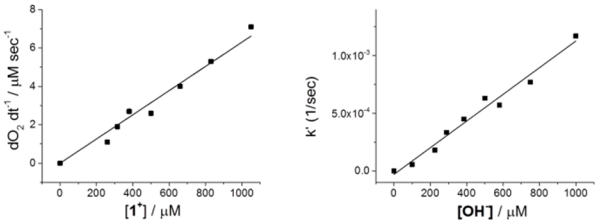

Figure 4. Left: Initial rate of O_2 production as a function of initial $[\mathbf{1A}^+]$ in excess NaOH (40 mM). Right: Pseudo-first order rate constants as a function of OH^- in excess $[1A^+]$ (2mM).

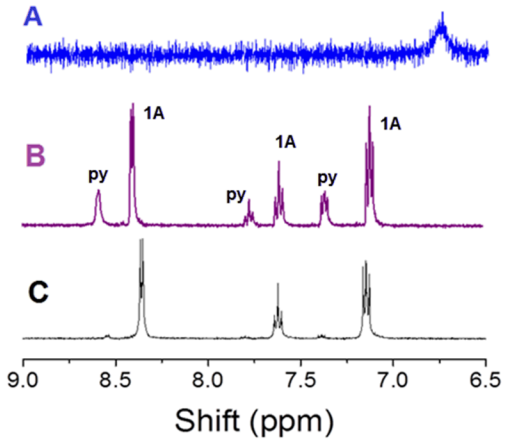

Figure 5. ^{1}H-NMR spectra of CD_3CN solutions of A) $\mathbf{1A}^+$ (blue), B) a mixture of pyridine and **1A** (purple), C) the reaction of 1.5 mM $\mathbf{1A}^+$ with 4 eq. OH^- (black).

The fates of the OAc^- and py ligands after reaction were monitored by ^{1}H-NMR spectroscopy. The pyridine region of the ^{1}H-NMR spectrum of $\mathbf{1A}^+$ in CD_3CN consists of a single broad peak, owing to the paramagnetic broadening of this material (Figure 5A). Upon addition of 4 eq. hydroxide (Figure 5C) the resulting spectrum most prominently contains sharp pyridine resonances that match those of **1A** (Figure 5B). Free pyridine and acetate resonances are observed above NMR detection limit only when using 1.5 mM or higher cubium concentrations (Figure 5C and Figure S2 respectively). Integration of the free:bound ligand ratio indicated 99.5% of ligands (py and OAc) remain bound to cubane **1A**. Free ligands were not seen in previous studies, which utilized cubane concentrations 5-150x less than that used here[49,54]. Collectively, these data suggest that the stoichiometric reduction reaction between cubium and OH- proceeds without net ligand loss.

High resolution mass spectrometry of the reaction products using ^{18}O-hydroxide were conducted to determine the origin of the evolved O_2. After dissolving $\mathbf{1A}^+$ in water (79% ^{18}O) containing 0.3M sodium bicarbonate (100% ^{18}O), the product *solution* was analyzed by ESI-QTOF-MS in positive ion mode (No negative ion peaks were observed). The MS spectrum (Figure S3) consisted of peaks at 875 m/z (**1A** + $^{23}Na)^+$, 853 (**1A**H)$^+$, 774 (**1A**-py + H^+) 796 (**1A**-py + $^{23}Na^+$), and 793 (**1A**-OAc)$^+$, and no evidence for ^{18}O incorporation into any fragment. Peaks at M+1 and M+2 for each fragment quantitatively account for the natural abundance of ^{13}C in each product (± 1%) and were completely consistent with control MS spectra of **1A** in either ^{16}O or ^{18}O water, with and without added ^{18}O bicarbonate (Figures S3-S5). Hence, **1A** is inert to µ-oxo/water exchange, and throughout the course of the O_2 evolving reaction of $\mathbf{1A}^+$ in bicarbonate no ^{18}O was incorporated into the bridging oxos. This outcome dictates that the oxygen atoms in the product O_2 must *both* originate from hydroxide, a prediction that was subsequently confirmed by membrane inlet mass spectrometry (MIMS).

MIMS allows real-time detection of O_2 produced from dissolution of $\mathbf{1A}^+$ in alkaline solution. The O_2 product from the dissolution of $\mathbf{1A}^+$ with ^{18}O bicarbonate in 97% ^{18}O-water under purged-Ar atmosphere was comprised of 75% $^{36}O_2$, 19% $^{34}O_2$ and 6% $^{32}O_2$ (Figure 6). In our setup, performing identi-

cal experiments with higher amounts of background air in the MS, causes the intensity of the $^{34}O_2$ signal to increase in direct correlation with a decrease in the $^{36}O_2$ signal (Figure S6). Therefore, a portion of the $^{34}O_2$ signal arises from scrambling of $^{36}O_2$ with atmospheric $^{32}O_2$ *via*: $^{32}O_2 + {}^{36}O_2 \rightarrow 2\ {}^{34}O_2$. Extrapolation to zero background air gives >81% $^{36}O_2$ as a lower bound percentage of the product O_2 yield.

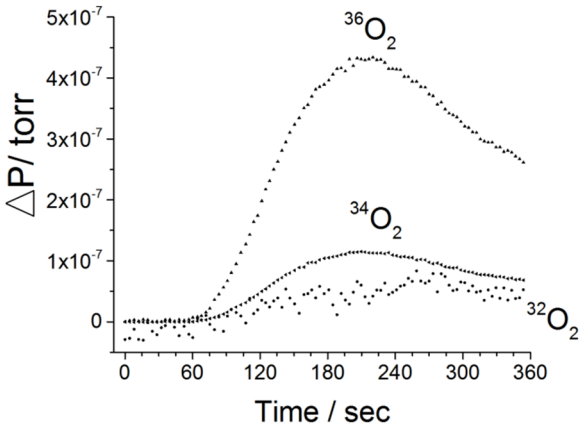

Figure 6. MIMS data for the reaction of **1A**+ (8mM) with ^{18}O labeled sodium bicarbonate (0.15 M) in 97% ^{18}O water.

The cumulative results suggest that the O_2 evolution reaction occurs by addition of OH^- without loss of ligands, and that these sites are eventually evolved as O_2 following oxidation by the $\mathbf{1A}^+/\mathbf{1A}$ couple (1.25 V vs. NHE). $\mathbf{1A}^+$ thus has unique, dual functionality depending on ligation, serving both as outer sphere oxidant and pre-catalyst.

DFT Calculations of Hydroxide Exchange

For further insights, we pursued DFT calculations to predict the energetics of formation of intermediates with progressive addition or exchange of ligands for water and hydroxide. Calculations were performed on an extended set of molecules (see Supporting Information) in acetonitrile solution on the geometries optimized in vacuo. To calculate the energetics of different reaction pathways, we employed fragments (OH^-, OAc^- and Py) solvated by four water molecules. Additional calculations employing four explicit water molecules in the solvation sphere of the reaction sites have been performed to further check the stability of different reaction intermediates. The calculated oxidation potential of the $\mathbf{1A}/\mathbf{1A}^+$ couple is 5.57 eV, vertical line in Figure 7, which nicely compares with the experimental oxidation potential of ~5.7 eV vs vacuum (i.e. 1.25 V vs. NHE +4.44 eV).

We consider two possible binding sites, i.e. exchange of OH- with a pyridine or insertion of OH^- into a Co-OAc bond to form a complex that is stabilized by a hydrogen bond to the monodentate acetate ligand, shown in Figure 7. Crystallographic evidence for intramolecular H bonding of this type has been directly observed in Mn_4O_4-cubanes,[62] and correlated with water oxidation activity in cobalt hangman complexes.[22] OH^- addition to the neutral cubane **1A,** forming anion $[\mathbf{1A}(OH)]^-$, is thermodynamically unfavored (+0.36 to 0.46 eV, at ^-OAc and Py sites; Figure 7). For the oxidized cubium $\mathbf{1A}^+$ the lowest energy pathway for OH^- addition is the associative product $[\mathbf{1A}(OH)]$, rather than by pyridine exchange (-0.92 vs. -0.63 eV, respectively, Figure 7). Intermediate $[\mathbf{1A}(OH)]$ has also been found lowest in energy by Li and Siegbahn[56] at the identical $Co_4(3,3,3,4)$ level.

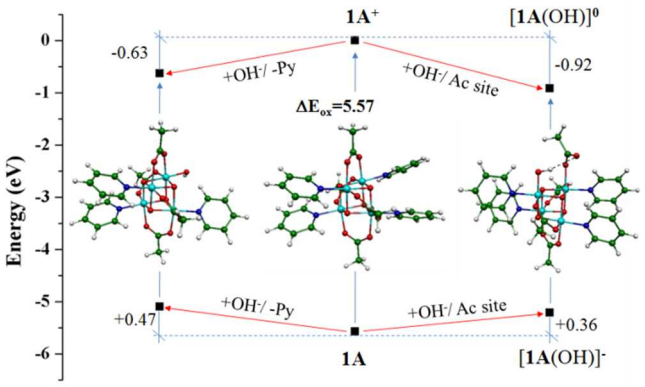

Figure 7. Stereochemistry and energetics from DFT calculations of intermediates for the first OH^- binding to both **1A** (unfavorable) and $\mathbf{1A}^+$(favorable). The calculated $\mathbf{1A}/\mathbf{1A}^+$ oxidation potential is also reported.

Li and Siegbahn assumed conditions of 1.43 V oxidizing potential[56] and calculated that $[\mathbf{1A}(OH)]^0$ is further oxidized to $Co_4(3,3,4,4)$. In their calculation, this derivative undergoes O-O bond formation *via* water nucleophilic attack. In our calculations, which limit the oxidizing potential to 1.25 V (equal to the couple $\mathbf{1A}/\mathbf{1A}^+$), oxidation of $[\mathbf{1A}(OH)]^0$ is unfavorable by +0.27 eV, and proton transfer from the hydroxide to the acetate ligand is highly unfavorable by +1.13 eV. We thus considered a second OH^-/H_2O binding as the next step in the reaction mechanism (Figure 8). Our calculations find it weakly unfavorable to replace a second pyridine ligand from $Co_4(3,3,3,4)$ with OH^- (+0.07 eV) or H_2O (+0.05 eV). Thus, the cubium likely retains at least 3 pyridine ligands throughout the catalytic mechanism. This agrees with the studies of Bonchio, et. al., who observed a direct correlation of electron transfer rates with the Hammett values of pyridine substituents[51].

We thus considered associative intermediates of general formula $[\mathbf{1A}(OH)_2]^{-1}$ in which a second OH- has inserted into one of the remaining seven Co-acetate bonds (Figure 8). One-electron oxidation of all of these isomers by $\mathbf{1A}^+$ is energetically favorable by 1.25-E^o > 0.15 eV, yielding a formal Co4(3,3,4,4) redox level. This oxidation level can also be represented as a Co^{3+}-bound peroxo in which the two bound OH- are oxidized and deprotonated, but this structural rearrangement is only feasible if the activation energy barriers for each isomer can be surmounted. Peroxo formation is greatly disfavored for the trans and gauche isomers in absence of rotational possibilities, which we are pursuing further. For the cis-type isomers, the OH^- ligands are separated by ~2.6 Å; this distance does not allow any appreciable O-O bond formation energy. In contrast, the gem-dihydroxo intermediate coordinates both OH on one Co and should have the lowest activation barrier to the peroxo intermediate of all dihydroxo intermediates. Our calculations cannot distinguish a preference for cis or gem-type intermediates, as these are isoenergetic in our most refined calculations to date (assuming four explicit water molecules in addition to the dielectric solvation model). Preliminary results also indicate similar stability of the ensuing peroxide-bound cubanes. Further, these in-

termediates are energetically degenerate (within <0.1 eV) with the corresponding oxo-aquo tautomers [(**1A**(O)(H_2O)]^{o} in triplet ground state in the dielectric solvation model (Figure S9). We note such intermediates require different O-O bond formation mechanisms, with the latter involving nucleophilic addition of a third OH^- to the Co^V=O. Both mechanisms have literature precedence, as water oxidation through a 1,1-gem-diol was proposed by Mattioli et al.[63], while Wang and Van Voorhis[57] reported coupling via a 1,2-cis-diol.

While our calculations currently cannot distinguish between the gem and cis intermediates in terms of energy, future calculations to predict the activation barriers for O-O bond formation may resolve this question. However, our experimental data provides clear guidance on this question. Our NMR data shows 0.5% (net) ligand dissociation occurs (carboxylate dissociation is required for the cis pathway) thus favoring the geminal pathway. Additional experimental evidence for the geminal pathway comes from our studies of the analogous cubium **1B**$^{3+}$, as described next.

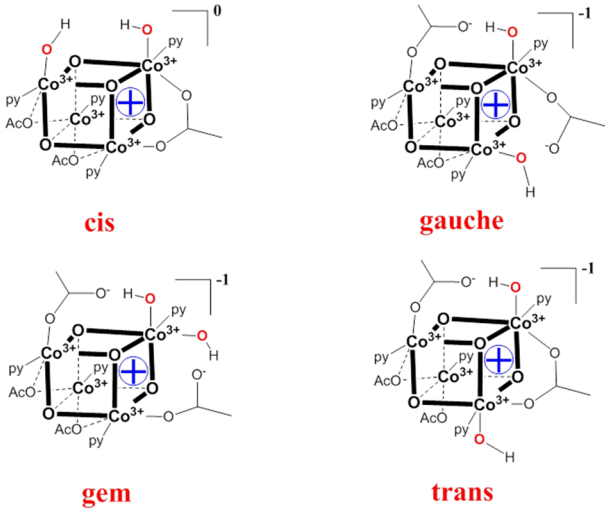

Figure 8. List of considered isomers of possible binding sites of second OH^-.

Reaction of 1B^{3+} with Hydroxide.

We pursued analogous experimental tests of cubium **1B**$^{3+}$. This derivative features a more positively charged cubane coordinated by 4 bidentate bpy and 2 bidentate OAc^- ligands in trans geometry (Scheme 1). Consequently, DFT calculations predict higher OH^- affinity for this derivative, with formation of the positively charged [cis-**1B**$(OH)_2]^+_{\text{-OAc}}$ complex favored by 0.30 eV relative to formation of the negatively charged [cis-**1A**$(OH)_2]^{-1}_{\text{-OAc}}$ species. **1B**$^{3+}$ shows a ~400 mV higher reduction potential than **1A**$^+$ in acetonitrile[54], but the measured electrochemical potentials are identical (1.25 V vs. NHE) in >pH 4 water[42,50]. Carboxylate exchange is known for both cubanes[35,54] and **1A** is known to bind water at these sites[60,61], suggesting bound water may contribute to this change in oxidizing potential.

A reported synthesis was used to isolate **1B**$(ClO_4)_3$ according to Christou et. al.[34] To our knowledge, the EPR signal has not been previously published, but has been described as a broad resonance at g= 2.20 with no resolved hyperfine. Our EPR spectrum (Figure S7) confirms this description and identifies the ground state spin S = ½. The shift of the g value (g > 2.0023) arising from Co spin-orbit coupling indicates a greater than half-filled 3d^n valence shell (n > 5). Analogous to **1A**$^+$, the absence of resolved ^{59}Co hyperfine splitting indicates the hole is delocalized onto the four μ_3-oxos of the $[Co_4O_4]^{5+}$ core, and the average spin density on any one Co is < 15%.

In sharp contrast to **1A**$^+$, no O_2 is produced from the reaction between **1B**$(ClO_4)_3$ and OH^-. This species does react but only CO_2 is produced, indicating bpy ligand oxidation. Bpy oxidation also occurs in pH neutral water: UV-Vis spectroscopy of aqueous **1B**$^{3+}$ solutions after aging for 1 hr show 12±3% reduction to cubane **1B**$^{2+}$ with no production of O_2 (Figure S8). No evidence of any reaction was observed in acidic solution (pH 0-2).

We derive two conclusions from these results. First, **1B**$(ClO_4)_3$ serves as a negative control in which the initial hydrolytic or oxidation intermediates are not reactive in water oxidation over bpy oxidation. Second, we infer one possible origin of the different water oxidation activities of **1A**$^+$ and **1B**$^{3+}$ as due to their different carboxylate stereochemistry. Only **1A**$^+$ can form the geminal-1,1 intermediate, while both **1A**$^+$ and **1B**$^{3+}$ can form the cis-1,2 intermediates depicted in Figure 8.

Discussion

The molecular Co_4O_4 cubane is inert for electrochemical oxidation of water to O_2 in aqueous phosphate buffer at pH 7[59–61]. This fact has been suggested by Nocera et al[59] as evidence that the cubane core is not a direct catalyst for water oxidation, but rather breakdown products or other Co contaminants may have been the pre-catalysts that formed active centers. The evidence presented here and recently by others[60,61] has shown this first observation is true because water cannot bind to Co centers in the cubane **1A** in competition with Py, OAc- and phosphate ligands. However, when water is ionized to hydroxide this stronger nucleophile is sufficient to form an inner sphere association complex with **1A** in higher yield which is a pre-catalyst to O_2 evolution. The results shown herein and by Tilley et al[61] extend that strategy by starting with the cationic cubium **1A**$^+$, thereby further favoring the association complex. Subsequent reaction with a second OH^- as shown kinetically[61] and indicated by our DFT calculations, leads to an intermediate that can now be oxidized by **1A**$^+$ resulting in O_2 evolution. This system may be analogous to that reported of Cronin, et. al., who observed O_2 evolution upon dissolution of heterogeneous Co^{IV}-oxides[64].

In agreement with Tilley et. al.[61] our results find a reaction of stoichiometry 4 **1A**$^+$ + 4 OH^- → O_2 + 4 **1A** + 2 H_2O with quantitative recovery of O_2 (75%, ref[61], vs. 100%, here) and **1A** (99.5%). The O_2 product originates from OH^- and not bridging oxos, as evidenced by QTOF-MS and MIMS (>81% doubly labeled O_2). O_2 produced via outer sphere oxidation of free hydroxide to OH● radical (1.8-2.0 V) is not possible energetically. Rather, our calculations also agree that OH^- insertion into Co-OAc^- binding sites is energetically preferential, as also predicted by Li and Siegbahn[56]. We find that insertion of two OH^- into Co-OAc^- sites, forming either 1,1(gem)-dihydro

or 1,2-dihydroxo intermediates, are energetically favorable pathways to form species that, thermodynamically, can be oxidized by **1A**$^{+}$ to yield either side-on ($\eta^{1,1}$-) or bridging ($\eta^{1,2}$-) peroxo intermediates, respectively.

Our kinetic studies, measured using saturating concentrations of OH^- and **1A**$^{+}$, fit well a simple first-order molecularity in each (R^2=0.98) and no improvement to the fit is made by introducing a second-order term (R^2=0.98). However, Tilley et al. [61] reported a faster time resolution kinetic study using stopped flow UV-Vis absorption, and showed the rate expression fits better to the sum of first and second order terms in **1A**$^{+}$ when non saturating concentrations are used. Our first-order rate constant (1.1) compares exceptionally well to that obtained by Tilley et. al. (0.8), confirming these studies are self-consistent. Neither we nor Tilley et. al. have observed any reaction intermediate directly. The proposed reaction mechanism by both groups is kinetically *identical*, only differing in terms of the description of the later intermediates. Both proposals involve associative addition of the first OH^- to **1A**$^{+}$ yielding intermediate [**1A**(OH)]^{o}.

The main mechanistic differences of our proposal compared to Li and Siegbahn[56] and Tilley et al[61] is that the second oxidation step to the formal $Co_4(3,3,4,4)$ cannot occur at the first hydroxide intermediate owing to insufficient redox energy for **1A**$^{+}$/**1A** , but becomes favorable after a second OH^- associates. Second, we find (via EPR) that electron-hole delocalization is a required feature of the mixed valence states rather than localized Co oxidation states. These features are emphasized in our proposed mechanism (Scheme 2). Here we propose that OH^- addition and one-electron oxidation (by a second eq. of **1A**$^{+}$), forms the di-hydroxo species, [**1A**$(OH)_2$]^{o} by concerted or stepwise reactions and is rate limiting for overall O_2 production.

We previously showed that neither trinuclear nor dinuclear Co(III) complexes prepared using the identical sets of ligands, py/OAc^- or bpy/OAc^-, exhibit activity in water oxidation[54]. This is attributed to their > 0.8 V higher reduction potential for the mixed valence Co(IV)/Co(III) couples. These non-cuboidal compounds lack the favorable delocalization energy unique to the molecular orbitals of the cubane topology, as evidenced both here and elsewhere by EPR spectroscopy.[44] Hence, the cubane structure allows stabilization of the $Co_4(3,3,4,4)$ oxidation state, from which a $Co_4(3,3,3,3)$-bound peroxide can be obtained. The production of O_2 from this step follows easily, as **1A**$^{+}$ is capable of oxidizing hydrogen peroxide[61].

Considering the absence of O_2 evolution from cubium **1B**$^{3+}$ which lacks geminal OAc^- ligands, we strongly favor the gem-1,1-dihydroxo pathway over the cis-1,2-dihydroxo pathway for O_2 evolution by **1A**$^{+}$. However, we cannot rule out other reasons for why **1B**$^{3+}$ is a poorer pre-catalyst. Competition between oxidation of bpy (CO_2 evolution) and OH^- oxidation, or slow kinetics due to charge repulsion between 2+ and 3+ cations could be two reasons why the yield of O_2 is zero.

With this mechanism established we can thus conclude that, under photochemical conditions using photo-generated oxidants ($Ru(bpy)_3^{3+}$, 1.26 V, and persulfate radical, 2.4 V), earlier reports[49–51,54] most likely observed a combination of O_2 produced catalytically from **1A** and Co^{2+} impurities. It is plausible that ligand dissociation to produce available water binding sites on cubane **1A** is more facile *under illumination*, rationalizing different observations seen between photochemical and electrochemical systems[59]. Precedence for this is known by the $Mn_4O_4(O_2PPh_2)_6$ cubane, which photodissociates phosphinate anion upon UV irradiation[65–68]. The apparent inactivity of a water oxidation catalyst candidate under one set of conditions thus cannot infer that the candidate will be inactive under all conditions.

Many observations reported here provide updated context for earlier reports[49–51,54] discussing catalysis from **1A**. Our data shows 0.5% ligand loss following a single turnover of **1A**$^{+}$/OH^-, in excellent agreement with literature showing <5% photo-decomposition of **1A** after 6-12 turnovers using $Ru(bpy)_3^{3+}$ and persulfate radicals[49]. The lack of O_2 evolution at pH 7 in the absence of buffer in this latter system[54] is now rationalized by the insufficient concentration of necessary OH^- substrate.

Scheme 2. Proposed mechanism of hydroxide oxidation by cubane complexes, building on concepts from this work and elsewhere[54].

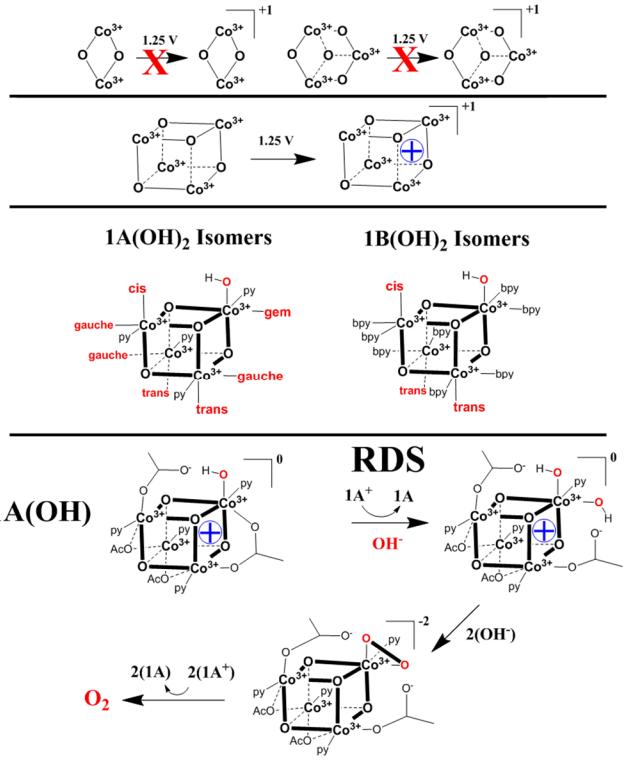

Our kinetic results rationalize the previous observation[54] that $Ru(bpy)_3^{3+}$ alone (1.26 V) could not generate O_2 from **1A** and water. This observation was reinforced by electrochemical results of several groups[49,51,59] (as well as Figure 1) which show little to no water oxidation current at applied potentials in that region. As measured here, pseudo-first order rate constants for hydroxide reaction with **1A**$^{+}$ are on the order of 10^{-4}-10^{-3} s^{-1} (Figure 4). Rates of $Ru(bpy)_3^{3+}$ decomposition by OH^- promoted hydrolysis are on the order of 10^{-3}-10^{-2} s^{-1}, as measured by Mallouk et al.[69]. Hence, hydroxide (if available) reacts with $Ru(bpy)_3^{3+}$ (typically in excess concentration) roughly an order of magnitude faster than with **1A**$^{+}$. When considering that all previous studies have utilized pH 7-8 (=

10^{-6}-10^{-7} M [OH^-]), millimolar concentrations of $\mathbf{1A}^+$ would yield rates approximately 10^{-9}-10^{-10} s^{-1} for O_2 evolution, as estimated by eqn. 2. Such rates are likely to be additionally affected by the presence of buffers which have been reported to compete for cobalt binding sites[70]. In particular, phosphate has been shown to inactivate[71] and inhibit[20] homogeneous cobalt catalysts by binding at sites for substrate OH^-.

Conclusion.

Effective heterogeneous oxidation catalysts such as spinel Co_3O_4 and cubic $LiCoO_2$ have lattices built around a Co_4O_4 cubane type structure[2,4,72]. This architecture is known to be important to allow thermodynamically accessible oxidation to Co^{4+}, as evidenced by the favorable oxidation potentials of the molecular clusters, $\mathbf{1A}/\mathbf{1A}^+$ and $\mathbf{1B}^{2+}/\mathbf{1B}^{3+}$, in contrast to the much higher Co^{III}/Co^{IV} oxidation potentials (~ 1 V higher) for $[Co_3O_4]^{2+}$ and $[Co_2O_2]^+$ model complexes with identical ligands.[54] These heterogeneous catalysts, at an oxidizing potential of 1.26 V ($Ru(bpy)_3^{3+}$), have pseudo-first order rate constants for O_2 evolution on the order of 10^{-2}-10^{-1}/s*Co (e.g, 0.019 for $LiCoO_2$ [ref4], 0.01 for Co_3O_4 [ref2], 0.5 for Co-M2P [ref15]).

With the assumption of similar rate laws to that reported here, the pseudo-first order rate constants we obtain at 1.25 V (10^{-4}-10^{-3}, Figure 4) indicate 10-1000x faster kinetics for water oxidation are afforded by efficient water/hydroxide binding. This comparison suggests that a molecular metal-oxo cubane architecture in a coordination environment of oxidatively stable ligands could achieve even faster turnover rates than homogeneous catalysts. While cubium $\mathbf{1B}^{3+}$ did not have stable organic ligand architecture, the acetates and pyridines are not oxidized in the case of $\mathbf{1A}^+$. Hence, this offers an optimistic future that molecular cobalt catalysts with organic ligands- if designed appropriately- may tolerate the harsh conditions needed to oxidize water and remain stable over useful lifetimes.

Lastly, when testing water oxidation catalysts with chemical oxidants, few are known[73] and each have tradeoffs: e.g., cerium ammonium nitrate has been challenged as noninnocent, [74] sodium periodate may donate substrate oxos, and $Ru(bpy)_3^{3+}$ is unstable. Here, pristine $\mathbf{1A}^+$ shows excellent aqueous stability at pH<7 ($\mathbf{1B}^{3+}$<pH4). Cubium couples appear to be innocent, outer-sphere one-electron redox mediator under acidic conditions.

Experimental.

Materials and Methods. All solutions were prepared with reagent grade water (18 MΩ, Hydro Picopure). All solvents and reagents were reagent grade, purchased commercially and used without further purification. $NaH^{13}C^{18}O_3$ bicarbonate was used to induce formation of $^{18}OH^-$ in experiments requiring isotopic labeling. ^{18}O water was purchased as 97% from Aldrich or 98% from Icon Isotopes. UV-Vis spectra were recorded on an HP-8452A Diode Array spectrophotometer in standard 1 cm pathlength quartz cells. EPR spectra were recorded on a Bruker ESP300 spectrometer equipped with Oxford cryostat model 900 at 10K. Samples were glasses of $\mathbf{1A}^+$ in acetonitrile and $\mathbf{1B}^+$ in 1M H_2SO_4. A CH Instruments Electrochemical Workstation was used for exhaustive electrolysis experiments.

A Clark type oxygen electrode (Hansatek Ltd) was used to obtain oxygen evolution data, and calibrated daily using N_2 deoxygenated and oxygen saturated atmospheric solutions. Clark electrode experiments were performed by monitoring the addition of 20μL of 1M NaOH to 500μL of 95/5 H_2O/CH_3CN solutions of $\mathbf{1A}^+$. The initial rates were obtained by determining the slope over the beginning linear region (~10s) of O_2 evolution.

Gas chromatography data were recorded on a Perkin Elmer Clarus 680 GC with a TCD detector (Ar carrier gas) operating at 40ºC (O2) or 200ºC (CO_2). Gas chromatography experiments monitored the addition of 200 μL of Ar-degassed 0.1 M NaOH to solid powders of $\mathbf{1A}^+$ or $\mathbf{1B}^{3+}$ in Ar-degassed 2 mL vials, and were adjusted using the N_2 signal as a control.

Membrane Inlet Mass Spectroscopy data were taken with a Stanford Research Systems CIS100 residual gas analyzer. A 1/16" capillary partially submerged in a dry ice/ethyleneglycol/ethanol trap @ -40ºC was used to connect the CIS to a KF/Swagelok adapter, in which sat a porous polyethylene support, a 12.5 μm Teflon membrane (Hansatech), and an O-ring. This assembly was clamped to the KF connection of a glass reaction vessel. Solid $\mathbf{1A}^+$ and ^{18}O bicarbonate were placed on top of the membrane while the vessel was Ar-purged, and ^{18}O was Ar-purged in its container as delivered. When ^{18}O water was added by syringe, nitrogen, CO_2 (labeled and unlabeled) and Argon were monitored in addition to the O_2 isotopes as control signals; the $^{32}O_2$ and $^{34}O_2$ signals were adjusted from the residual N_2 signal in the resulting data. The $^{36}O_2$ signal was adjusted from the background Ar signal in the resulting data. All O_2 signals adjust for separate background signals before injection. For MS data>100 amu, spectra were recorded by direct injection of nM samples via syringe pump into an Agilent 6510 QTOF LC/MS running in dual ESI mode.

Syntheses. 1A was prepared as previously described[49,54]. Purification was performed by collecting the first, green fraction off a column of silica gel using 5% methanol/dichloromethane mobile phase. $\mathbf{1ACl}O_4$ ($\mathbf{1A}^+$) was made by bulk electrolysis (1.1-1.2V) of a 0.4M $LiClO_4/CH_3CN$ solution of **1A**, followed by reduction of solvent volume to ~5ml by rotary evaporation, addition of water (~35 ml), and overnight refrigeration, giving a precipitate collected by filtration in 10-15% yield. A porous carbon rod (working), Ti wire (counter) and silver wire (pseudoreference) were used as electrodes; the latter two electrodes were compartmentalized in fritted glass tubes (Ace glass) filled only with blank electrolyte (no cobalt). $\mathbf{1A}^+$ as the PF_6 salt was prepared exactly as described in ref[59].

$\mathbf{1B}^{2+}$ as a perchlorate salt was prepared as described[54] as the salt which precipitates following CH3CN electrolysis of $\mathbf{1B}^{2+}$ at 1.5 V vs. Ag pseudoreference.

Computational details. All the calculations have been performed by the Gaussian 09 program package[75]. We optimized all the molecular structures using the B3LYP exchange–correlation functional[76] and a 6-311G* basis set[77,78] in vacuo. The solvation effects are evaluated by the conductor-like polarizable continuum model (C-PCM),[79,80] using acetonitrile as a solvent. To calculate the energetics of the reaction path-

ways, we used fragments (OH^-, OAc^- and Py) including four explicit water molecules in acetonitrile.

ASSOCIATED CONTENT

Supporting Information

9 figures including QTOF-MS and raw DFT data. This material is available free of charge via the Internet at http://pubs.acs.org.

Corresponding Author

*dismukes@rutgers.edu

ACKNOWLEDGMENT

This work was supported by the Air Force Office of Scientific Research (FA9550-11-1-0231). Fellowships were provided by NSF-IGERT (P.F.S., DGE 0903675), NSF CLP #1213772 (S.K.), Rutgers University (A.L.) the Lawrenceville School, Lawrenceville, NJ (L.H.), CAPES Brazil 13386/13-1 (K.U.D.C), and BASF (V.S.). We are grateful to Drs. A. Ermakov, G. K. Kumaraswamy and A. Tyryshkin for instrumentation support and to Dr. Y. Geletii, Dr. M. Symes, G. Gardner, and C. Kaplan for helpful discussions. The authors declare no competing financial interests.

REFERENCES

(1) Shafirovich, V. Y.; Strelets, V. V. *Nouv. J. Chim.* **1977**, *2*, 199–201.
(2) Jiao, F.; Frei, H. *Angew. Chemie-International Ed.* **2009**, *48*, 1841–1844.
(3) Brunschwig, B. S.; Chou, M. H.; Creutz, C.; Ghosh, P.; Sutin, N. *J. Am. Chem. Soc.* **1983**, *105*, 4832–4833.
(4) Gardner, G. P.; Go, Y. B.; Robinson, D. M.; Smith, P. F.; Hadermann, J.; Abakumov, A.; Greenblatt, M.; Dismukes, G. C. *Angew. Chemie* **2012**, *124*, 1648–1651.
(5) Suzuki, O.; Takahashi, M.; Fukunaga, T.; Kuboyama, J. US Patent 3399966, 1968.
(6) El Wakkad, S. E. S.; Hickling, A. *Trans. Faraday Soc.* **1950**, *46*, 820–824.
(7) Kanan, M. W.; Nocera, D. G.; Kana, M. W. *Science (80-.).* **2008**, *321*, 1072–1075.
(8) Hutchings, G. S.; Zhang, Y.; Li, J.; Yonemoto, B. T.; Zhou, X.; Zhu, K.; Jiao, F. *J. Am. Chem. Soc.* **2015**, *137*, 4223–4229.
(9) Gerken, J. B.; McAlpin, J. G.; Chen, J. Y. C.; Rigsby, M. L.; Casey, W. H.; Britt, R. D.; Stahl, S. S.; Rigsby, L.; Casey, W. H.; Britt, R. D.; Stahl, S. S. *J. Am. Chem. Soc.* **2011**, *133*, 14431–14442.
(10) Nocera, D. G. *Acc. Chem. Res.* **2012**, *45*, 767–776.
(11) Risch, M.; Ringleb, F.; Chernev, P.; Zaharieva, I.; Dau, H. *Energy Environ. Sci.* **2015**, 661–674.
(12) Risch, M.; Klingan, K.; Ringleb, F.; Chernev, P.; Zaharieva, I.; Fischer, A.; Dau, H. *ChemSusChem* **2012**, *5*, 542–549.
(13) Du, P.; Kokhan, O.; Chapman, K. W.; Chupas, P. J.; Tiede, D. M. *J. Am. Chem. Soc.* **2012**, *134*, 11096–11099.
(14) Zhong, M.; Hisatomi, T.; Kuang, Y.; Zhao, J.; Liu, M.; Iwase, A.; Jia, Q.; Nishiyama, H.; Minegishi, T.; Nakabayashi, M.; Shibata, N.; Niishiro, R.; Katayama, C.; Shibano, H.; Katayama, M.; Kudo, A.; Yamada, T.; Domen, K. *J. Am. Chem. Soc.* **2015**, *137*, 5053–5060.
(15) Koroidov, S.; Anderlund, M. F.; Styring, S.; Thapper, A.; Messinger, J. *Energy Environ. Sci.* **2015**, *8*, 2492–2503.
(16) Li, Y.; Zhang, L.; Torres-Pardo, A.; González-Calbet, J. M.; Ma, Y.; Oleynikov, P.; Terasaki, O.; Asahina, S.; Shima, M.; Cha, D.; Zhao, L.; Takanabe, K.; Kubota, J.; Domen, K. *Nat Commun* **2013**, *4*, 2566.
(17) Kanan, M. W.; Surendranath, Y.; Nocera, D. G. *Chem. Soc. Rev.* **2009**, *38*, 109–114.
(18) Zhong, D. K.; Cornuz, M.; Sivula, K.; Gratzel, M.; Gamelin, D. R. *Energy Environ. Sci.* **2011**, *4*, 1759–1764.
(19) Han, X. B.; Zhang, Z. M.; Zhang, T.; Li, Y. G.; Lin, W.; You, W.; Su, Z. M.; Wang, E. B. *J. Am. Chem. Soc.* **2014**, *136*, 5359–5366.
(20) Wang, D.; Groves, J. T. *Proc. Natl. Acad. Sci.* **2013**, *110* , 15579–15584.
(21) Wasylenko, D. J.; Ganesamoorthy, C.; Borau-Garcia, J.; Berlinguette, C. P. *Chem. Commun.* **2011**, *47*, 4249–4251.
(22) Dogutan, D. K.; McGuire, R.; Nocera, D. G. *J. Am. Chem. Soc.* **2011**, *133*, 9178–9180.
(23) Shevchenko, D.; Anderlund, M. F.; Thapper, A.; Styring, S. *Energy Environ. Sci.* **2011**, *4*, 1284–1287.
(24) Rigsby, M. L.; Mandal, S.; Nam, W.; Spencer, L. C.; Llobet, A.; Stahl, S. S. *Chem. Sci.* **2012**, *3*, 3058.
(25) Evangelisti, F.; Güttinger, R.; Moré, R.; Luber, S.; Patzke, G. R. *J. Am. Chem. Soc.* **2013**, *135*, 18734–18737.
(26) Yin, Q.; Tan, J. M. J. M.; Besson, C.; Geletii, Y. V; Musaev, D. G.; Kuznetsov, A. E.; Luo, Z.; Hardcastle, K. I.; Hill, C. L. *Science (80-.).* **2010**, *328*, 342–345.
(27) Pizzolato, E.; Natali, M.; Posocco, B.; Montellano Lopez, A.; Bazzan, I.; Di Valentin, M.; Galloni, P.; Conte, V.; Bonchio, M.; Scandola, F.; Sartorel, A.; Montellano López, A. *Chem. Commun.* **2013**, *49*, 9941–9943.
(28) Leung, C.-F.; Ng, S.-M.; Ko, C.-C.; Man, W.-L.; Wu, J.; Chen, L.; Lau, T.-C. *Energy Environ. Sci.* **2012**, *5*, 7903.
(29) Lv, H.; Song, J.; Geletii, Y. V; Vickers, J. W.; Sumliner, J. M.; Musaev, D. G.; Kögerler, P.; Zhuk, P. F.; Bacsa, J.; Zhu, G.; Hill, C. L. *J. Am. Chem. Soc.* **2014**, *136*, 9268–9271.
(30) Swiegers, G. F.; Clegg, J. K.; Stranger, R. *Chem. Sci.* **2011**, *2*, 2254–2262.
(31) Sartorel, A.; Bonchio, M.; Campagna, S.; Scandola, F. *Chem. Soc. Rev.* **2013**, *42*, 2262–2280.
(32) Dismukes, G. C.; Brimblecombe, R.; Felton, G. A. N.; Pryadun, R. S.; Sheats, J. E.; Spiccia, L.; Swiegers, G. F. *Acc. Chem. Res.* **2009**, *42*, 1935–1943.
(33) Blakemore, J. D.; Crabtree, R. H.; Brudvig, G. W. *Chem. Rev.* **2015**. **DOI:** 10.1021/acs.chemrev.5b00122
(34) Dimitrou, K.; Brown, A. D.; Concolino, T. E.; Rheingold, A. L.; Christou, G. *Chem. Commun.* **2001**, 1284–1285.
(35) Dimitrou, K.; Folting, K.; Streib, W. E.; Christou, G. *J. Am. Chem. Soc.* **1993**, *115*, 6432–6433.
(36) Dimitrou, K.; Sun, J.-S. S.; Folting, K.; Christou, G. *Inorg. Chem.* **1995**, *34*, 4160–4166.
(37) Dimitrou, K.; Folting, K.; Streib, W. E.; Christou, G. *J. Chem. Soc. Chem. Commun.* **1994**, *838*, 1385–1386.
(38) Chakrabarty, R.; Bora, S. J.; Das, B. K. *Inorg. Chem.* **2007**, *46*, 9450–9462.
(39) Chakrabarty, R.; Sarmah, P.; Saha, B.; Chakravorty, S.; Das, B. K. *Inorg. Chem.* **2009**, *48*, 6371–6379.
(40) Sarmah, P.; Chakrabarty, R.; Phukan, P.; Das, B. K. *J. Mol. Catal. A Chem.* **2007**, *268*, 36–44.
(41) Das, B. K.; Chakrabarty, R. *J. Chem. Sci.* **2011**, *123*, 163–173.
(42) Symes, M. D.; Surendranath, Y.; Lutterman, D. a.; Nocera, D. G. *J. Am. Chem. Soc.* **2011**, *133*, 5174–5177.
(43) Symes, M. D.; Lutterman, D. A.; Teets, T. S.; Anderson, B. L.; Breen, J. J.; Nocera, D. G. *ChemSusChem* **2013**, *6*, 65–69.
(44) McAlpin, J. G.; Stich, T. A.; Ohlin, C. A.; Surendranath, Y.; Nocera, D. G.; Casey, W. H.; Britt, R. D. *J. Am. Chem. Soc.* **2011**, *133*, 15444–15452.
(45) Stich, T.; Krzystek, J.; Mercardo, B. Q.; McAlpin, J. G.; Ohlin, C. A.; Olmstead, M. M.; Casey, W. H.; Britt, R. D. *Polyhedron* **2013**, *64*, 304–307.
(46) McAlpin, J. G.; Surendranath, Y.; Dincă, M.; Stich, T. A.; Stoian, S. A.; Casey, W. H.; Nocera, D. G.; Britt, R. D. *J. Am. Chem. Soc.* **2010**, *132*, 6882–6883.
(47) Beattie, J. K.; Hambley, T. W.; Klepetko, J. a.; Masters, A. F.; Turner, P. *Polyhedron* **1998**, *17*, 1343–1354.
(48) Sumner, C. E. *Inorg. Chem.* **1988**, *27*, 1320–1327.
(49) McCool, N. S.; Robinson, D. M.; Sheats, J. E.; Dismukes, G.

C. *J. Am. Chem. Soc.* **2011**, *133*, 11446–11449.
(50) La Ganga, G.; Puntoriero, F.; Campagna, S.; Bazzan, I.; Berardi, S.; Bonchio, M.; Sartorel, A.; Natali, M.; Scandola, F. *Faraday Discuss.* **2012**, *155*, 177.
(51) Berardi, S.; Natali, M.; Bazzan, I.; Puntoriero, F.; Sartorel, A.; Scandola, F.; Campagna, S.; Bonchio, M. *J. Am. Chem. Soc.* **2012**, *134*, 11104–11107.
(52) Zhang, B.; Li, F.; Yu, F.; Wang, X.; Zhou, X.; Li, H.; Jiang, Y.; Sun, L. *ACS Catal.* **2014**, 804–809.
(53) Zhou, X.; Li, F.; Li, H.; Zhang, B.; Yu, F.; Sun, L. *ChemSusChem* **2014**, *7*, 2453–2456.
(54) Smith, P. F.; Kaplan, C.; Sheats, J. E.; Robinson, D. M.; McCool, N. S.; Mezle, N.; Dismukes, G. C. *Inorg. Chem.* **2014**, *53*, 2113–2121.
(55) La Ganga, G.; Nardo, V. M.; Cordaro, M.; Natali, M.; Vitale, S.; Licciardello, A.; Nastasi, F.; Campagna, S. *Dalt. Trans.* **2014**, *43*, 14926–14930.
(56) Li, X.; Siegbahn, P. E. M. *J. Am. Chem. Soc.* **2013**, *135*, 13804–13813.
(57) Wang, L. P.; Van Voorhis, T. *J. Phys. Chem. Lett.* **2011**, *2*, 2200–2204.
(58) Fernando, A.; Aikens, C. M. *J. Phys. Chem. C* **2015**, *119*, 11072–11085.
(59) Ullman, A. M.; Liu, Y.; Huynh, M.; Bediako, D. K.; Wang, H.; Anderson, B. L.; Powers, D. C.; Breen, J. J.; Abruña, H. D.; Nocera, D. G. *J. Am. Chem. Soc.* **2014**, *136*, 17681–17688.
(60) Sartorel, A.; Genoni, A.; LaGanga, giuseppina; Volpe, A.; Puntoriero, F.; Di Valentin, M.; Bonchio, M.; Natali, M. *Faraday Discuss.* **2015. DOI: 10.1039/C5FD00076A**.
(61) Nguyen, A. I.; Ziegler, M. S.; Oña-Burgos, P.; Sturzbecher-Hohne, M.; Kim, W.; Bellone, D. E.; Tilley, T. D. *J. Am. Chem. Soc.* **2015**. 137, 12865-12872.
(62) Wu, J. Z.; Sellitto, E.; Yap, G. P. A.; Sheats, J.; Dismukes, G. C. *Inorg. Chem.* **2004**, *43*, 5795–5797.
(63) Mattioli, G.; Giannozzi, P.; Amore Bonapasta, A.; Guidoni, L. *J. Am. Chem. Soc.* **2013**, *135*, 15353–15363.
(64) Bloor, L. G.; Molina, P. I.; Symes, M. D.; Cronin, L. *J. Am. Chem. Soc.* **2014**, *136*, 3304–3311.
(65) Ruettinger, W.; Yagi, M.; Wolf, K.; Bernasek, S.; Dismukes, G. C. *J. Am. Chem. Soc.* **2000**, *122*, 10353–10357.
(66) Wu, J. Z.; De Angelis, F.; Carrell, T. G.; Yap, G. P. A.; Sheats, J.; Car, R.; Dismukes, G. C. *Inorg. Chem.* **2006**, *45*, 189–195.
(67) Brimblecombe, R.; Swiegers, G. F.; Dismukes, G. C.; Spiccia, S. *Angew. Chem. Int.* **2008**, *47*, 7335–7338.
(68) Brimblecombe, R.; Kolling, D. R. J.; Bond, A. M.; Dismukes, G. C.; Spiccia, L.; Swiegers, G. F. *Inorg. Chem.* **2009**, *48*, 7269–7279.
(69) Hara, M.; Waraksa, C. C.; Lean, J. T.; Lewis, B. A.; Mallouk, T. E. *J. Phys. Chem. A* **2000**, *104*, 5275–5280.
(70) Liu, H.; Schilling, M.; Yulikov, M.; Luber, S.; Patzke, G. R. *ACS Catal.* **2015**, 4994–4999.
(71) Davenport, T. C.; Ahn, H. S.; Ziegler, M. S.; Tilley, T. D. *Chem. Commun.* **2014**, *50*, 6326–6329.
(72) Cady, C. W.; Gardner, G.; Maron, Z. O.; Retuerto, M.; Go, Y. B.; Segan, S.; Greenblatt, M.; Dismukes, G. C. *ACS Catal.* **2015**, 3403–3410.
(73) Parent, A. R.; Crabtree, R. H.; Brudvig, G. W. *Chem. Soc. Rev.* **2013**, *42*, 2247–2252.
(74) Demars, T. J.; Bera, M. K.; Seifert, S.; Antonio, M. R.; Ellis, R. J. *Angew. Chemie Int. Ed.* **2015**, *54*, 7534–7538.
(75) Frisch, M. J.; Trucks, G. W.; Schlegel, H. B.; Scuseria, G. E.; Robb, M. A.; Cheeseman, J. R.; Scalmani, G.; Barone, V.; Mennucci, B.; Petersson, G. A.; Nakatsuji, H.; Caricato, M.; Li, X.; Hratchian, H. P.; Izmaylov, A. F.; Bloino, J.; Zheng, G.; Sonnenberg, J. L.; Hada, M.; Ehara, M.; Toyota, K.; Fukuda, R.; Hasegawa, J.; Ishida, M.; Nakajima, T.; Honda, Y.; Kitao, O.; Nakai, H.; Vreven, T.; Montgomery, J. A., Jr.; Peralta, J. E.; Ogliaro, F.; Bearpark, M.; Heyd, J. J.; Brothers, E.; Kudin, K. N.; Staroverov, V. N.; Kobayashi, R.; Normand, J.; Raghavachari, K.; Rendell, A.; Burant, J. C.; Iyengar, S. S.; Tomasi, J.; Cossi, M.; Rega, N.; Millam, J. M.; Klene, M.; Knox, J. E.; Cross, J. B.; Bakken, V.; Adamo, C.; Jaramillo, J.; Gomperts, R.; Stratmann, R. E.; Yazyev, O.; Austin, A. J.; Cammi, R.; Pomelli, C.; Ochterski, J. W.; Martin, R. L.; Morokuma, K.; Zakrzewski, V. G.; Voth, G. A.; Salvador, P.; Dannenberg, J. J.; Dapprich, S.; Daniels, A. D.; Farkas, Ö.; Foresman, J. B.; Ortiz, J. V.; Cioslowski, J.; Fox, D. J. Gaussian 09, Revision A.1; Gaussian, Inc.: Wallingford, CT, 2009.
(76) Becke, A. D. *J. Chem. Phys.* **1993**, *98*, 5648–5652.
(77) McLean, A. D.; Chandler, G. S. *J. Chem. Phys.* **1980**, *72*, 5639–5648.
(78) Krishnan, R.; Binkley, J. S.; Seeger, R.; Pople, J. A. *J. Chem. Phys.* **1980**, *72*, 650–654.
(79) Cossi, M.; Rega, N.; Scalmani, G.; Barone, V. *J. Comput. Chem.* **2003**, *24*, 669–681.
(80) Cossi, M.; Barone, V. *J. Chem. Phys.* **2001**, *115*, 4708–4717.

TOC Artwork

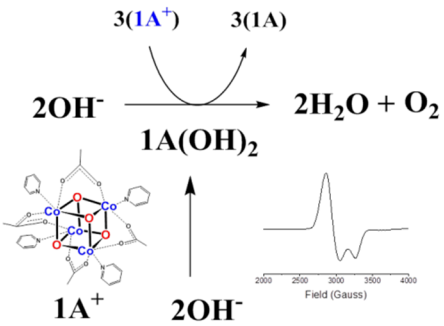
3(1A+)
3(1A)
2OH-
2H2O + O2
1A(OH)2
1A+
2OH-
2000
2500
3000
3500
4000
Field (Gauss)